Period2 3′-UTR and microRNA-24 regulate circadian rhythms by repressing PERIOD2 protein accumulation

Seung-Hee Yoo[a,b,1], Shihoko Kojima[b,2], Kazuhiro Shimomura[c,3], Nobuya Koike[b,d], Ethan D. Buhr[c,4], Tadashi Furukawa[c,5], Caroline H. Ko[c,6], Gabrielle Gloston[a], Christopher Ayoub[a], Kazunari Nohara[a], Bryan A. Reyes[e], Yoshiki Tsuchiya[d], Ook-Joon Yoo[f], Kazuhiro Yagita[d], Choogon Lee[g], Zheng Chen[a], Shin Yamazaki (山崎　晋)[e,7], Carla B. Green[b], and Joseph S. Takahashi[b,h,1]

[a]Department of Biochemistry and Molecular Biology, The University of Texas Health Science Center at Houston, Houston, TX 77030; [b]Department of Neuroscience, The University of Texas Southwestern Medical Center, Dallas, TX 75390; [c]Department of Neurobiology, Northwestern University, Evanston, IL 60208; [d]Department of Physiology and Systems Bioscience, Kyoto Prefectural University of Medicine, Kyoto 602-8566, Japan; [e]Department of Biological Sciences, Vanderbilt University, Nashville, TN 37235-1634; [f]Graduate School of Medical Science and Engineering, Korea Advanced Institute of Science and Technology, Daejeon 305-701, Korea; [g]Program in Neuroscience, Department of Biomedical Sciences, College of Medicine, Florida State University, Tallahassee, FL 32306; and [h]Howard Hughes Medical Institute, The University of Texas Southwestern Medical Center, Dallas, TX 75390

Contributed by Joseph S. Takahashi, September 7, 2017 (sent for review April 21, 2017; reviewed by Paul E. Hardin, Satchin Panda, and Hiroki R. Ueda)

We previously created two PER2::LUCIFERASE (PER2::LUC) circadian reporter knockin mice that differ only in the *Per2* 3′-UTR region: *Per2::Luc*, which retains the endogenous *Per2* 3′-UTR and *Per2::LucSV*, where the endogenous *Per2* 3′-UTR was replaced by an SV40 late poly(A) signal. To delineate the in vivo functions of *Per2* 3′-UTR, we analyzed circadian rhythms of *Per2::LucSV* mice. Interestingly, *Per2::LucSV* mice displayed more than threefold stronger amplitude in bioluminescence rhythms than *Per2::Luc* mice, and also exhibited lengthened free-running periods (∼24.0 h), greater phase delays following light pulse, and enhanced temperature compensation relative to *Per2::Luc*. Analysis of the *Per2* 3′-UTR sequence revealed that miR-24, and to a lesser degree miR-30, suppressed PER2 protein translation, and the reversal of this inhibition in *Per2::LucSV* augmented PER2::LUC protein level and oscillatory amplitude. Interestingly, *Bmal1* mRNA and protein oscillatory amplitude as well as CRY1 protein oscillation were increased in *Per2::LucSV* mice, suggesting rhythmic overexpression of PER2 enhances expression of *Per2* and other core clock genes. Together, these studies provide important mechanistic insights into the regulatory roles of *Per2* 3′-UTR, miR-24, and PER2 in *Per2* expression and core clock function.

Per2 gene | circadian | miR-24 | microRNA | 3′-UTR regulation

Virtually all living organisms have evolved an intrinsic timing system, the circadian clock, to anticipate and exploit daily environmental changes. Circadian clocks commonly display three cardinal features, namely, a circadian free-running period, entrainment to environmental cues, and temperature compensation of circadian periodicity (1). These features allow the clocks to run on a consistent daily schedule, but on the other hand also confer adaptation to various environmental cues such as light, food, and temperature to achieve biological homeostasis and well-being (2, 3). In mammals, the clock system is organized in a hierarchical manner, with the central pacemaker in the hypothalamic suprachiasmatic nuclei (SCN) coordinating peripheral tissue clocks to perform essential physiological functions (4).

The mammalian cell-autonomous molecular oscillator consists of interlocked feedback loops (5). In the core loop, the positive transcription factors CLOCK and BMAL1 form heterodimers to drive the E-box enhancer-dependent transcription of *Cryptochrome* (*Cry*) and *Period* (*Per*) genes. The CRY and PER proteins in turn heterodimerize and translocate to the nucleus to inhibit CLOCK/BMAL1 activity. PER proteins are generally believed to play an auxiliary role in transcriptional repression (6), required for nuclear translocation of the primary repressor CRY (7–10). However, accumulating evidence also supports a coactivator function of PER in circadian transcription (11–14), suggesting complex molecular mechanisms. In the secondary loop, BMAL1 also drives the nuclear receptor *Rev-Erb* expression, and reciprocally *Bmal1* is tightly regulated by REV-ERBs and their opposing nuclear receptor RORs (15, 16). These nuclear receptors are thought to compete for binding to the shared element RORE and thus play important roles in circadian amplitude regulation (17). More recent studies have also shown amplitude regulatory mechanisms distinct from the competitive binding model (18, 19), suggesting an integrated control of circadian amplitude by diverse pathways.

Expression and activity of core clock factors are subject to posttranscriptional and posttranslational regulation (20–26). One emerging regulatory mechanism is microRNA (miRNA)-mediated mRNA degradation or translational repression (27). miRNAs are small noncoding RNAs that bind to target 3′ untranslated regions

Significance

The circadian oscillator is a cell-autonomous biological timer driving daily physiological rhythms to ensure fitness and health. Regulatory mechanisms of the oscillator are complex and not fully understood. We previously generated two circadian reporter mouse lines that differ only in the 3′-UTR region of the core clock gene *Per2*. Interestingly, substitution of the endogenous *Per2* 3′-UTR with an SV40 late poly(A) signal led to a lengthened period, enhanced PER2 protein level, and more robust oscillatory amplitude. PER2 also displayed a positive role in circadian transcription. Molecular and genetic studies showed the microRNA miR-24 binds to the *Per2* 3′-UTR to attenuate rhythmic PER2 accumulation. These results identified an important posttranscriptional regulatory mechanism of PER2 expression required for normal circadian timekeeping.

Author contributions: S.-H.Y., C.B.G., and J.S.T. designed research; S.-H.Y., S.K., K.S., N.K., E.D.B., T.F., C.H.K., G.G., C.A., K.N., B.A.R., Y.T., and S.Y. performed research; C.L. contributed new reagents/analytic tools; S.-H.Y., O.-J.Y., K.Y., S.Y., and C.B.G. analyzed data; and S.-H.Y., Z.C., and J.S.T. wrote the paper.

Reviewers: P.E.H., Texas A & M University; S.P., Salk Institute for Biological Science; and H.R.U., RIKEN Quantitative Biology Center.

The authors declare no conflict of interest.

Freely available online through the PNAS open access option.

[1]To whom correspondence may be addressed. Email: Seung-Hee.Yoo@uth.tmc.edu or joseph.takahashi@utsouthwestern.edu.

[2]Present address: Department of Biological Sciences and Biocomplexity Institute, Virginia Tech, Blacksburg, VA 24061.

[3]Present address: Department of Neurology, Northwestern University, Feinberg School of Medicine, Chicago, IL 60611.

[4]Present address: Vision Science Center, Department of Ophthalmology, University of Washington School of Medicine, Seattle, WA 98109.

[5]Present address: Medicinal Safety Research Laboratories, Daiichi Sankyo Co., Ltd., Edogawa-ku, Tokyo 134-8630, Japan.

[6]Present address: Department of Chemistry, Northwestern University, Evanston, IL 60208.

[7]Present address: Department of Neuroscience, The University of Texas Southwestern Medical Center, Dallas, TX 75390.

This article contains supporting information online at www.pnas.org/lookup/suppl/doi:10.1073/pnas.1706611114/-/DCSupplemental.

(3′-UTRs) of mRNAs via sequence-specific interaction, regulating mRNA stability and/or translational efficiency (28). Together, miRNAs target a majority of protein-coding genes involved in various physiological processes. In particular, global knockout of *Dicer*, encoding the enzyme responsible for cleaving pre-miRNA to generate miRNAs, significantly shortened the circadian activity period (29), providing genetic evidence that miRNAs collectively play a regulatory role in clock function. Several other studies have also investigated specific miRNAs that regulate expression of core clock components (27, 30–32). For example (33), miR-132 and miR-219 were previously identified as enriched in mouse SCN neurons, displaying light-inducible and circadian expression requiring CREB and CLOCK/BMAL1, respectively. Functional analysis further revealed their respective activity to diminish light-responsive phase delay and shorten circadian period length, at least in part involving *Per1* activation. These studies together suggest a pervasive miRNA regulation of the clock that requires further mechanistic understanding.

We previously generated *Per2::Luc* reporter mice where the luciferase coding sequence was inserted before the endogenous *Per2* stop codon such that expression of PER2::LUC fusion proteins is driven by the natural *Per2* promoter (34, 35). This reporter mouse line has proven highly versatile, allowing direct visualization of robust molecular rhythms of PER2 as a state variable of the circadian clock. Consistent with a normal circadian function of PER2::LUC, the reporter line showed indistinguishable behavioral and molecular characteristics compared with the wild-type (WT) mice (34). Using these mice, we showed that peripheral tissues are self-sustained, SCN-independent oscillators, and the SCN coordinates the phases of peripheral oscillators (34). We produced a modified version of reporter mice, *Per2::LucSV*, that harbors a replacement of the endogenous *Per2* 3′-UTR with an SV40 poly(A) signal, and fibroblast cells derived from these mice were previously reported (36, 37). To investigate the regulation and function of *Per2* in vivo, particularly its 3′-UTR, we conducted in-depth molecular and behavioral studies of *Per2::LucSV* mice. Our results revealed a regulatory role of miR-24 and *Per2* 3′-UTR in *Per2* expression and provided in vivo evidence for a positive transcription function of PER2 in the circadian oscillator leading to amplitude enhancement.

Results

Generation and Circadian Characterization of *Per2::LucSV* Knockin Mice. We previously generated the *Per2::Luc* reporter knockin mouse line with an intact endogenous *Per2* 3′-UTR (34). To investigate the role of *Per2* 3′-UTR in mRNA half-life and translational regulation, we created a modified knockin version expressing PER2::LUC. Specifically, the endogenous 3′-UTR of the original *Per2::Luc* knockin targeting vector (34) was replaced with an SV40 poly(A) signal sequence. The short arm for homologous recombination from the original vector was also changed to a 3.1-kb genomic DNA region 3 kb downstream from the original short arm used for *Per2::Luc* knockin (Fig. 1*A*). The presence of the correctly targeted *Per2::LucSV* allele was confirmed by Southern blotting analysis and PCR (Fig. S1 *A* and *B*). Intercrosses between heterozygous (C57BL/6J × 129S6SvEvTac) F_1 offspring produced WT, heterozygous *Per2::LucSV* knockin, and homozygous F_2 animals at the expected 1:2:1 Mendelian ratio. Mice heterozygous and homozygous for the targeted allele were developmentally and morphologically indistinguishable from WT littermates.

To begin to determine the effect of the *Per2::LucSV* allele on the circadian clock, we first analyzed the circadian behavior of *Per2::LucSV* mice. Unlike the previous *Per2::Luc* reporter mice (34), which showed normal behavioral periodicity compared with WT (23.69 ± 0.07), *Per2::LucSV* mice displayed longer free-running periods in constant darkness (DD) (23.91 ± 0.06, $n = 12$, t test: $^*P < 0.0001$) (Fig. 1*B*). Furthermore, they also exhibited greater phase delays than WT when light pulse was administrated at CT17 (Fig. 1*B*). Together, these results suggest a functional role of the *Per2* 3′-UTR in the circadian clock.

A Regulatory Role of 3′-UTR in PER2 Level and Oscillatory Amplitude. To delineate the circadian function of *Per2* 3′-UTR, we compared circadian rhythms between *Per2::Luc* and *Per2::LucSV* via real-time recording of bioluminescence from the SCN explants. *Per2::Luc* and *Per2::LucSV* mice were entrained to 12:12 light/dark (LD) cycles and SCN tissues were isolated 1 h before lights off. Whole-field bioluminescence from SCN slices was captured by camera and image stacks were then analyzed using the CellCycle program (Actimetrics). Interestingly, bioluminescence level and oscillatory amplitude in *Per2::LucSV* SCN explants were higher than those from *Per2::Luc* (Fig. 1*C* and Fig. S1*C* and Movie S1). Next we compared circadian bioluminescence rhythms in SCN and various peripheral tissues via photomultiplier tubes (PMTs) as previously described (34). All tissue explants from *Per2::LucSV* showed more robust and sustained circadian bioluminescence rhythms compared with those from *Per2::Luc* explants, characterized by three- to four-fold amplitude enhancement and elevated baseline levels. *Per2::LucSV* also showed tissue-specific period lengths that are significantly longer than in *Per2::Luc* in all tissues tested (Fig. 2). We derived mouse embryonic fibroblasts (MEFs) from both mouse lines, and reporter bioluminescence from MEFs also showed patterns consistent with the tissue explants. The robust and sustained bioluminescence in *Per2::LucSV* MEFs (Fig. S2) has been previously exploited for sensitive single-cell imaging and high-throughput screening (36, 37).

Effects of the *Per2* 3′-UTR Replacement on Core Clock Gene Repression. To explore how the *Per2* 3′-UTR substitution with the SV40 poly (A) affects clock gene expression, we determined both mRNA and protein expression patterns for several core clock genes in cerebellum and liver samples from *Per2::Luc* and *Per2::LucSV* mice maintained in constant darkness. Compared with the significantly enhanced bioluminescence, *Per2* mRNA level increase in *Per2::LucSV* relative to *Per2::Luc* was more modest and temporally restricted (Fig. 3*A*). Moreover, whereas *Cry1* mRNA oscillation was not significantly altered in cerebellum and liver of *Per2::LucSV*, *Bmal1* mRNA level increased significantly during subjective daytime in *Per2::LucSV* cerebellum and liver compared with *Per2::Luc* (Fig. 3*A*). In accordance with bioluminescence measurements (Fig. 2), the *Per2* 3′-UTR replacement caused markedly elevated PER2::LUC protein level and circadian amplitude throughout the circadian cycle in both cerebellum and liver (Fig. 3*B*). Therefore, a posttranscriptional mechanism was primarily responsible for the PER2 protein accumulation to which transcriptional control may also contribute. Although *Cry1* mRNA level was not significantly altered in *Per2::LucSV* (Fig. 3*A*), CRY1 protein level was increased in both tissues, suggesting that increased PER2::LUC protein levels promote CRY1/2 protein expression and/or stability (Fig. 3*C* and Fig. S3*A*). BMAL1 protein level increased during subjective daytime in *Per2::LucSV* cerebellum and liver compared with *Per2::Luc* (Fig. 3*D*). *Rev-Erbα* mRNA level was reduced in *Per2::LucSV* compared with *Per2::Luc* at CT4 (Fig. S3*B*), suggesting increased PER2::LUC protein level in *Per2::LucSV* at CT0 and CT4 may repress E-box–driven *Rev-Erbα* transcription, which in turn contributes to increased *Bmal1* transcription. These results together suggested that enhanced circadian amplitude and baseline level of PER2 augment the mRNA and/or protein oscillation of core clock components, including *Cry1* and *Bmal1*.

MicroRNA Regulation of PER Translation. To delineate the underlying molecular mechanism for increased PER2::LUC protein levels in *Per2::LucSV* mice, we first measured *Per2* mRNA half-life using actinomycin D-treated *Per2::Luc* and *Per2::LucSV* MEF cells. *Per2::Luc* mRNA half-life was estimated to be 0.45 h and 0.67 h in *Per2::Luc* and *Per2::LucSV* MEFs, respectively.

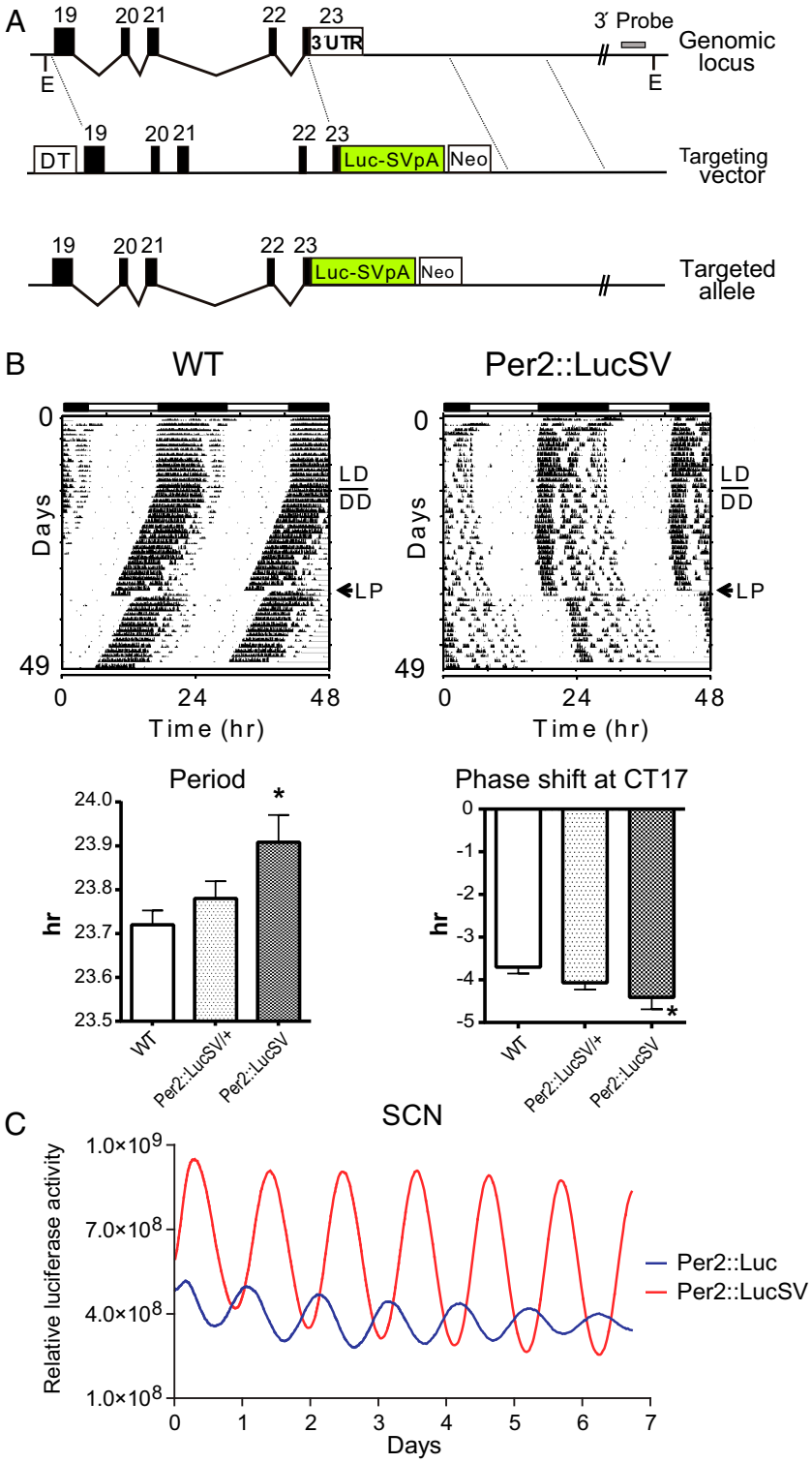

Fig. 1. Generation and circadian characterization of *Per2::LucSV* knockin mice. (*A*) Diagram of the mouse *Per2* locus, targeting vector, and targeted knockin allele. Exons are indicated by filled blocks with numbers. DT, diphtheria toxin A chain; E, EcoRI; Neo, neomycin resistance gene; triangle, loxP site. (*B*) Representative locomotor activity records from WT and *Per2::LucSV* homozygous knockin mice (WT, $n = 10$; *Per2::LucSV*, $n = 12$). Animals were maintained on LD12:12 for the first 14 d, indicated by the filled and empty bars above the records, before being transferred to DD to measure free-running periods. The free-running period of *Per2::LucSV* homozygous knockin mice was significantly longer than that of WT mice (*t* test: $^*P < 0.0001$). On day 20 in DD conditions, a 6-h light pulse (LP; arrow) was administered at circadian time 17. *Per2::LucSV* homozygous knockin mice showed greater phase delay compared with WT mice (*t* test: $^*P < 0.001$). WT, $n = 10$; *Per2::LucSV*/+, $n = 15$; *Per2::LucSV*, $n = 12$. (*C*) SCN explants were placed on an inverted microscope (DMI6000B, Leica) within an environmentally controlled Lucite chamber (Solent Scientific) maintained at 36 °C. Cultures were placed on a 36 °C Peltier heated stage within the chamber and tissues were imaged using a camera cooled to −20 °C (Stanford Photonics). Images were collected at 15 fps and threshold was applied to eliminate artifactual signals in real time. Images were subsequently integrated and analyzed by using the CellCycle program (Actimetrics), which can track single-cell images and quantify bioluminescence signals. Representative imaging data from *Per2::Luc* and *Per2::LucSV* heterozygous mouse SCN cultures with subtracted baseline are indicated as blue and red traces, respectively.

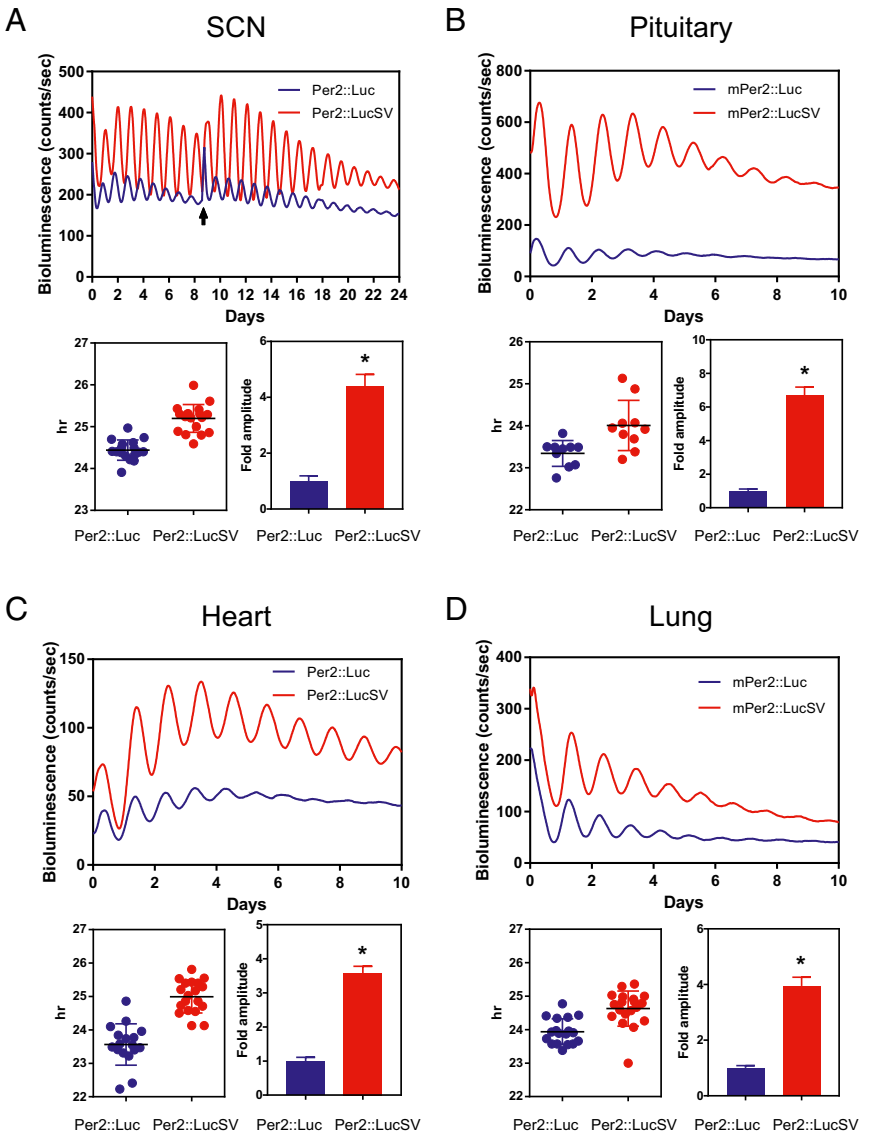

Fig. 2. Enhanced amplitude and baseline level of real-time bioluminescence rhythms in *Per2::LucSV* compared with *Per2::Luc*. Representative PER2::LUC bioluminescence recording of SCN (*A*), pituitary (*B*), heart (*C*), and lung (*D*) from *Per2::Luc* and *Per2::LucSV* homozygous mice. Mice were kept in a light/dark cycle before dissection. Tissue sections were harvested just before lights off and immediately cultured for recording. Arrow indicates a medium change (*A*). Recordings are neither normalized nor corrected for baseline drift. Blue and red traces represent PER2 rhythm from *Per2::Luc* and *Per2::LucSV* mice, respectively. For each tissue period and relative amplitude, comparisons are shown in the graphs *Below*. Relative fold amplitude of Per2::Luc and Per2::LucSV tissues were calculated by the LM fit (damped sin) method (lumicycle analysis, Actimetrics). In all four tissues, relative amplitude was significantly higher in *Per2::LucSV* (*t* test: $*P < 0.0001$). Error bars represent SD. *Per2::Luc* SCN mean circadian period: 24.44 ± 0.05885 ($n = 17$), *Per2::LucSV* SCN mean circadian period: 25.20 ± 0.07833 ($n = 18$). *t* test: *P* value < 0.0001 (*A*). *Per2::Luc* pituitary mean circadian period: 23.34 ± 0.09702 ($n = 10$), *Per2::LucSV* pituitary mean circadian period: 24.01 ± 0.1894 $n = 10$. *t* test: *P* value 0.0059 (*B*). *Per2::Luc* heart mean circadian period: 23.56 ± 0.1500 ($n = 17$), *Per2::LucSV* heart mean circadian period: 24.99 ± 0.1114 ($n = 19$). *t* test: *P* value < 0.0001 (*C*). *Per2::Luc* lung mean circadian period: 23.94 ± 0.09045 ($n = 18$), *Per2::LucSV* lung mean circadian period: 24.63 ± 0.1205 ($n = 19$). *t* test: *P* value < 0.0001 (*D*).

This result indicated that replacement of the endogenous 3′-UTR with the SV40 poly(A) sequence moderately stabilized the mRNA (Fig. 4*A*). In addition, *Bmal1* mRNA half-life was not affected by the *Per2* 3′-UTR change (Fig. S4*A*).

As mentioned above, while the PER2::LUC protein level was highly elevated throughout the circadian cycle in *Per2::LucSV* cerebellum and liver compared with *Per2::Luc*, the increase in *Per2::LucSV* mRNA amount was more modest and limited to certain time points (Fig. 3*A*). To investigate the primary cause for the increased PER2::LUC protein accumulation, we measured the poly(A) length of *Per2::Luc* mRNA in *Per2::Luc* and *Per2::LucSV* mouse liver using a poly(A) tail-length (PAT) assay (38–40). To our surprise, the poly(A) length of *Per2::Luc* mRNA was longer in *Per2::Luc* than in *Per2::LucSV*, indicating that increased PER2::LUC protein accumulation in *Per2::LucSV* was not due to poly(A) length change (Fig. 4*B*).

Next, we investigated whether any *cis*-regulatory elements in the *Per2* 3′-UTR were altered in *Per2::LucSV*, which might be responsible for PER2::LUC protein accumulation. We generated five reporter constructs containing serial truncations in the *Per2* 3′-UTR. Luciferase activity was significantly increased when the 3′-UTR fragment +1,232 to +1,932 was deleted (Fig. 4*C*). We analyzed this sequence using the TargetScanMouse algorithm (41) and identified five putative miRNA binding sites.

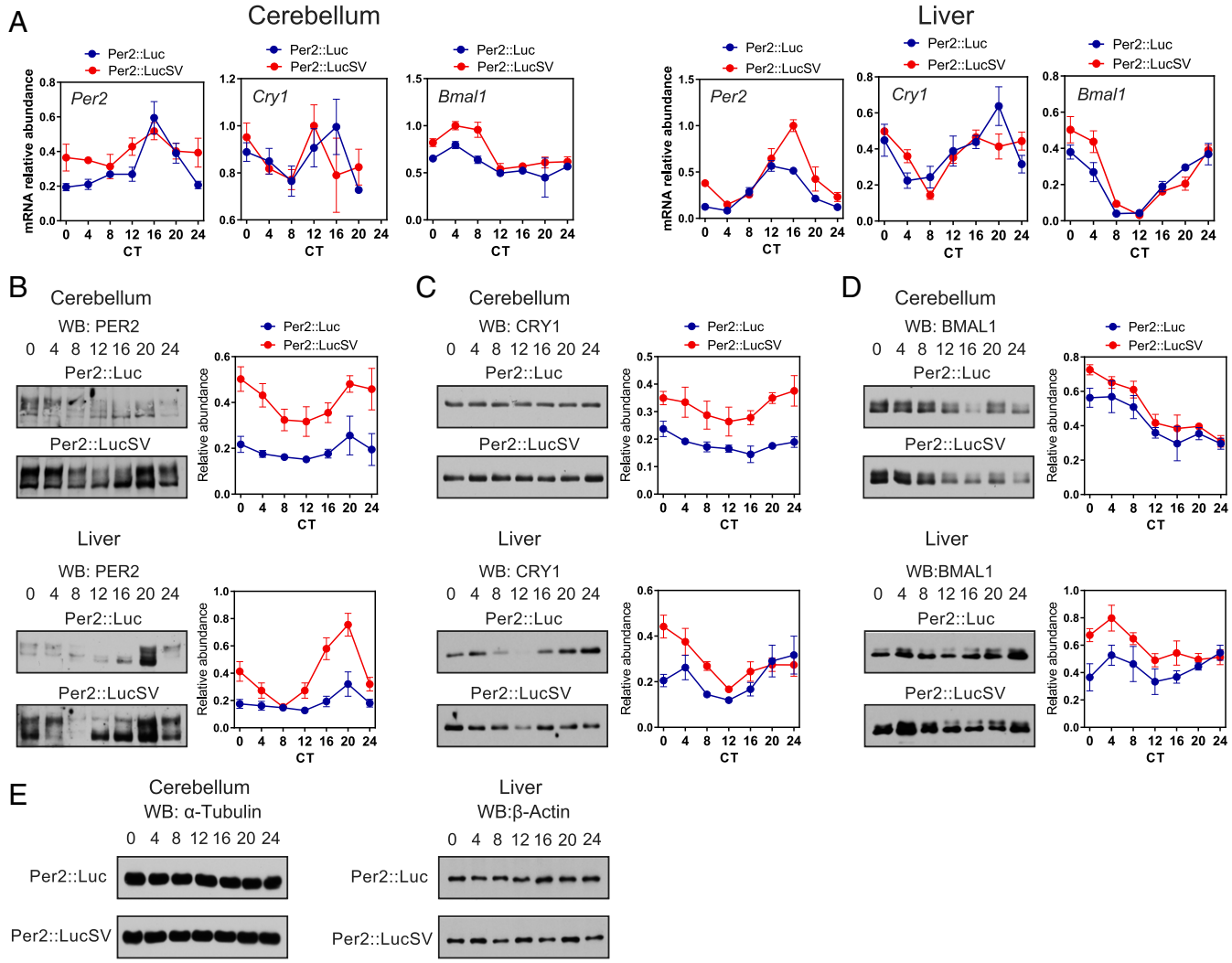

Fig. 3. Circadian genes display enhanced amplitude of mRNA and protein oscillation in *Per2::LucSV* cerebellum and liver. (*A*) Real-time RT-PCR analysis of clock gene expression in *Per2::Luc* and *Per2::LucSV* homozygous mice. Blue and red circles represent *Per2::Luc* and *Per2::LucSV* mice, respectively. Error bars represent SEM for each time point from three independent homozygous repeats. Two-way ANOVA shows significant statistical differences between *Per2::Luc* and *Per2::LucSV* mice for *Per2* (cerebellum and liver, $P < 0.0001$) *Bmal1* (cerebellum, $P < 0.0001$, liver, $P < 0.01$). (*B–D*) PER, CRY1, and BMAL1 protein oscillation in cerebellum (*Upper Left*) and liver (*Lower Left*). Quantification from the three independent experiments is shown to the *Right* of each representative. Blue and red circles represent values from *Per2::Luc* and *Per2::LucSV* mice. Error bars represent SEM ($n = 3$). Two-way ANOVA shows significant statistical differences between *Per2::Luc* and *Per2::LucSV* mice for PER2 (cerebellum and liver, $P < 0.0001$), CRY1 (cerebellum, $P < 0.0001$; liver, $P < 0.01$), BMAL1 (cerebellum, $P < 0.05$; liver, $P < 0.001$). (*E*) Actin Western blot from cerebellum and liver of *Per2::Luc* and *Per2::LucSV* homozygous mice.

Individual seed sequences for miRNA binding sites were mutated in the no. 5 3′-UTR construct and reporter assays were performed by using NIH 3T3 cells. Compared with the WT control (WT-5), the miR-24 binding site mutant clone (miR24-1686 mut) displayed significantly enhanced luciferase activity (Fig. 4*D*), suggesting a regulatory role of miR-24 in *Per2* expression. A mutation in the miR-30 site (miR30a-1602 mut) also induced luciferase activity as previously reported (29), albeit to a much lesser degree compared with the miR-24 mutation (Fig. 4*D*). When we introduced double mutations for both miR-24 and miR-30a binding sites in the 3′-UTR, an additive effect was observed in reporter assays (Fig. 4*E*).

We next transfected *Per2::Luc* MEF cells with either miRNA inhibitor or mimic oligonucleotides and monitored real-time PER2::LUC bioluminescence (Fig. 4*F*). MEF cells transfected with the miR-24 inhibitor oligonucleotide phenocopied *Per2::LucSV* and showed increased amplitude for the luciferase rhythm. Conversely, miR-24 mimic oligonucleotides decreased the reporter rhythm amplitude, together suggesting miR-24 plays an inhibitory role in PER2 protein expression. We further tested inhibitor oligonucleotides of several other candidate miRNAs, including miR-21, miR-25, and miR-30, and they did not potentiate the PER2::LUC rhythm in *Per2::Luc* MEFs. Next, we performed qPCR to determine the effect of miR-24 mimic on *Per2* mRNA level (Fig. 4*G*). Relative to control oligonucleotides, transfection of miR-24 mimic significantly reduced *Per2* mRNA level in *Per2::Luc* MEF cells, suggesting miR-24 alters PER2 protein level by destabilizing *Per2* mRNA, at least in part. We also performed qPCR analysis to investigate whether miR-24 expression is under circadian control. miR-24 expression was not rhythmic in cerebellum and liver, and cerebellum showed significantly higher miR-24 expression than liver (Fig. S4*B*).

Positive Transactivation Role of PER2 for Its Own Transcription. Somewhat surprisingly, based on the above analysis of E-box–driven transcription of *Per2* and *Cry1*, increased PER2::LUC

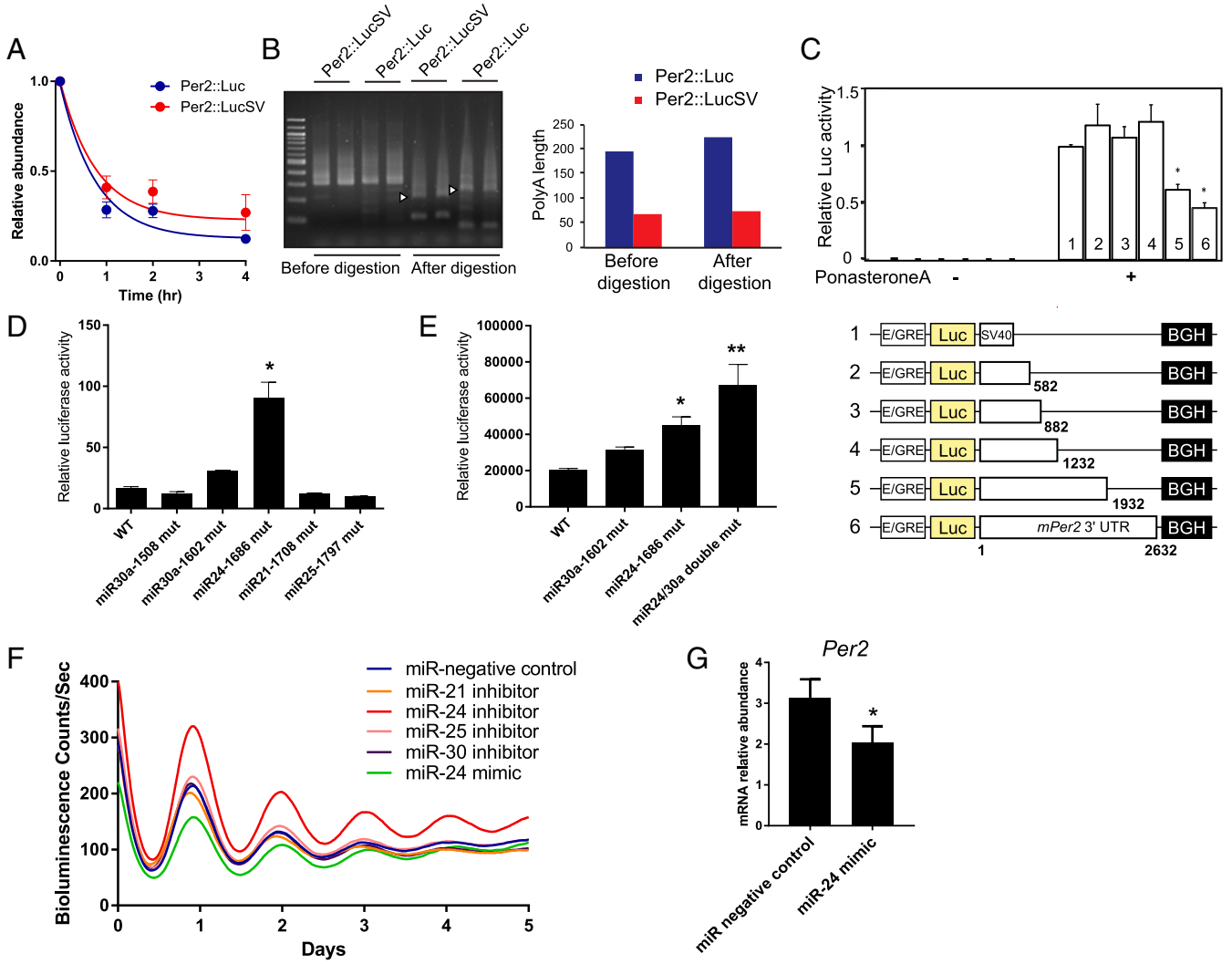

Fig. 4. miR-24 regulates *Per2* mRNA stability and protein translation. (*A*) *Per2* mRNA half-life measurement. MEFs generated from mPer2::Luc and mPer2::LucSV homozygous mice were plated 2 d before treatment with 2 μg/mL actinomycin D for the indicated periods of time. Total RNA was isolated from the harvested cells, and quantitative PCR was performed using firefly luciferase primers. Blue and red circles represent values from *Per2::Luc* and *Per2::LucSV* MEFs. Error bars represent SEM for each time point from three independent repeats. The half-life of *Per2::Luc* mRNA from *Per2::Luc* and *Per2::LucSV* MEFs was determined to be 0.45 h (blue) and 0.67 h (red), respectively. The half-life parameter K (rate constant) is not significantly different; $P = 0.314$ based on model-based nonlinear one-phase exponential decay analysis (GraphPad Prism 7). (*B*) The poly(A) tail length of *Per2* mRNA at ZT12 in the liver of *Per2::Luc* or *Per2::LucSV* mice. Ligation-mediated (LM)-PATs were performed and a representative gel image is shown. Each lane represents an individual mouse ($n = 2$). Arrowheads indicate the fragment derived after restriction enzyme treatment for poly(A) length measurement. Graph on the *Right* represents the poly(A) tail length calculated from the LM-PAT gel shown on the *Left*. (*C*) Serial truncation in the mouse *Per2* 3′-regulatory region were incorporated into a luciferase reporter construct containing an ecdysone-inducible expression system. BGH, BGH poly(A) signal; E/GRE, ecdyson/glucocorticoid responsive element; Luc, Luciferase; SV40, SV40 poly(A) signal. An equal amount of each reporter DNA construct was transiently transfected into NIH 3T3 cells with or without ponasterone A. Numbers at the *Right* of each construct indicate the end positions of the insert from the stop codon. Each value is the mean ± SEM of three replicates from three independent assays. The value of construct 1 was set as 1 for normalization. *$P < 0.005$ compared with the construct 1 (Student's *t* test). (*D*) Putative microRNA binding sites (*miR30a*, *miR-24*, *miR21*, and *miR25*) located between constructs 4 and 5 (1,232–1,932 bp) were mutated individually from construct 5, and 1–1,932 bp 3′-UTR with mutant miRNA sites were used to replace the SV40 poly(A) signal sequence. Two hundred nanograms of each reporter construct was transfected into NIH 3T3 cells. Each value is the mean ± SEM of three replicates. The results shown are representative of three independent experiments. The miR-24 site mutation caused significant reporter activation (one-way ANOVA for all three independent experiments: *$P < 0.0001$). (*E*) The binding sites for *miR-24* and *miR-30a* were mutated. Two hundred nanograms of each reporter construct was transfected into NIH 3T3 cells. Each value is the mean ± SEM of three replicates. The results shown are representative of three independent experiments. The miR-24/30a binding site double mutation showed an additive effect for reporter activation compared with WT (one-way ANOVA: *$P < 0.001$, **$P < 0.0001$ for the representative results, for two other experiments, miR24-1686 and miR24/30 double: $P < 0.0001$). (*F*) Amplitude of the circadian reporter rhythm was increased in *Per2::Luc* MEFs treated with miR-24 inhibitor oligonucleotides. Representative PER2::LUC bioluminescence recording from MEFs transfected with miRNA negative control (blue), miR-24 inhibitor (red) and miR-24 mimic (green), miR-25 mimic (pink), miR-30 mimic (purple), and miR-21 mimic (orange) are shown. (*G*) *Per2* mRNA amount was reduced by miR-24 mimic transfection in *Per2::Luc* MEFs (*t* test: *$P < 0.01$).

protein levels in *Per2::LucSV* mouse did not impose greater transcriptional inhibition in the core loop. Furthermore, *Bmal1* transcription was augmented during the subjective daytime in *Per2::LucSV* tissues, suggesting a positive role of PER2::LUC protein in circadian transcription. Consistent with other reports indicating PER2 as a coactivator for its own transcription (11, 13, 42), reporter assays using a *Per2* promoter construct showed potent stimulatory effects of *Per2* cotransfection on CLOCK/BMAL1-dependent transcriptional induction (Fig. 5*A*). PER2 expression not only enhanced CLOCK/BMAL1 transactivation but also

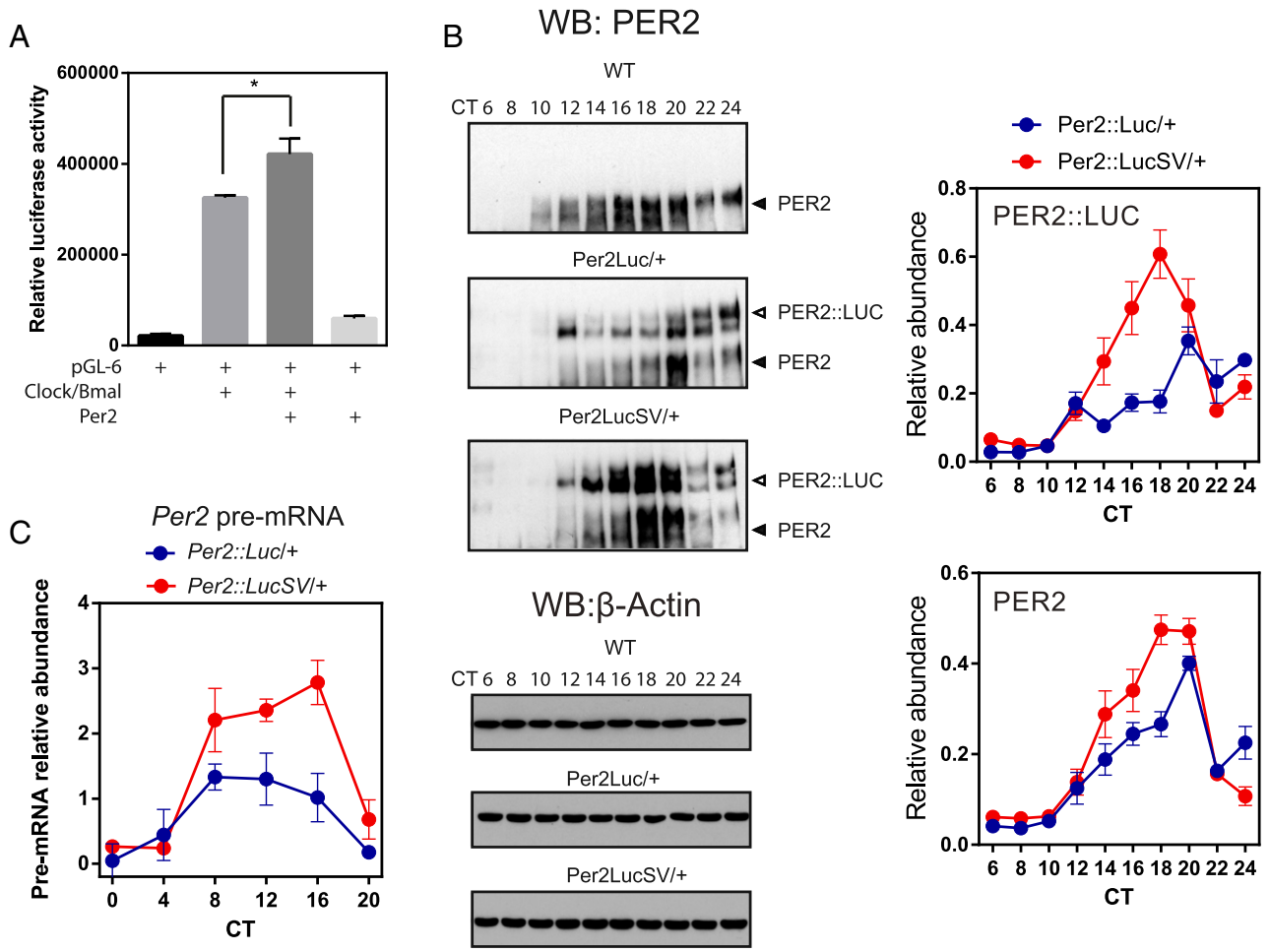

Fig. 5. PER2 functions as a positive regulator for *Per2* transcription in vitro and in vivo. (*A*) The mouse *Per2* promoter reporter construct pGL6 was transiently cotransfected into 293A cells with the indicated expression constructs. CLOCK/BMAL1-mediated transcriptional activation was significantly increased by PER2 coexpression (*F* test to compare variances, $F = 40.74$, $P = 0.04$). (*B*) Oscillation of PER2 (WT) and PER2::LUC fusion protein in liver. Western blotting was performed using liver protein extracts with the PER2 antibody. Both PER2 from the WT allele and PER2::LUC from the knockin allele were increased in the liver extract from *Per2::LucSV* heterozygous mice. Quantification for PER2::LUC (*Upper*) and PER2 (*Lower*) is shown at *Right*. Two-way ANOVA shows significant statistical differences in PER2::LUC and PER2 levels between *Per2::Luc*/+ and *Per2::LucSV*/+ mice; $P < 0.0001$. (*C*) Real-time RT-PCR analysis of *Per2* pre-mRNA in liver from *Per2::Luc* heterozygous (*Per2::Luc*/+) and *Per2::LucSV* heterozygous (*Per2::LucSV*/+) mice. Error bars represent SEM for each time point from three independent repeats. Two-way ANOVA shows significant differences between *Per2::Luc* heterozygous and *Per2::LucSV* heterozygous ($P < 0.0001$).

increased the baseline reporter activity in the absence of *Clock*/*Bmal1* cotransfection (Fig. 5*A*).

To determine effects of knockin alleles on transcription and translation of the endogenous *Per2* allele, we collected liver tissues at the indicated CT from *Per2::Luc* and *Per2::LucSV* heterozygous mice. Western blotting analysis showed that circadian expression of PER2::LUC protein was significantly enhanced from the *Per2::LucSV* allele relative to the *Per2::Luc* allele, due to the 3′-UTR replacement in the former and consequently removal of the endogenous miRNA binding sites (Fig. 5*B*, *Left Middle* and *Lower* panels of PER2 WB; quantification: *Upper Right*). Importantly, PER2 protein expression from the WT allele in *Per2::LucSV* heterozygote mouse liver was significantly elevated compared with that in *Per2::Luc* heterozygote mice (Fig. 5*B*, *Left Middle* and *Lower* panel of PER2 WB; quantification: *Lower Right*), and a similar pattern was observed for CRY1 in liver (Fig. S5*A*) and PER2 in kidney (Fig. S5*B*). These results strongly suggested that increased PER2::LUC protein expression from the *Per2::LucSV* allele may in turn activate *Per2* transcription. We next determined transcription initiation rate by measuring *Per2* pre-mRNA levels via qPCR analysis. From CT8 to CT20, the levels of *Per2* pre-mRNA was significantly elevated in *Per2::LucSV* relative to *Per2::Luc*, indicating an activating role of PER2 protein in the transcription of the endogenous *Per2* allele (Fig. 5*C*).

In a recent study (29), global *Dicer* knockout, as well as simultaneous knockdown of three PER1/2-targeting miRNAs including miR-24 and miR-30a, was found to shorten the circadian period lengths in cells and mice, contrary to the period-lengthening effect observed in *Per2::LucSV* mice. To delineate the role of PER2 and cognate miRNAs specifically, we analyzed an independent BAC transgenic (TG) mouse model of PER2 rhythmic overexpression, namely the *455N18BAC Per2* TG mice. Consistent with *Per2::LucSV*, we again observed lengthened circadian periods (Fig. 6*A*). *Per2* mRNA and protein expression was highly elevated in the *455N18BAC* TG mice compared with WT (Fig. 6 *B* and *C*). *Bmal1* expression was also markedly enhanced in the TG mice compared with WT (Fig. 6*C*, *Right*), again consistent with what we previously observed from *Per2::LucSV* mice (Fig. 3*C*). Interestingly, *Rev-Erbα* level was significantly reduced in *455N18BAC* TG mice at CT4 and CT8 compared with WT (Fig. S6). Consistent with results in Fig. S3*B*, this observation suggested that increased PER2 protein level potentiates *Bmal1* transcription by repressing REV-ERBα transcription. These results further affirmed

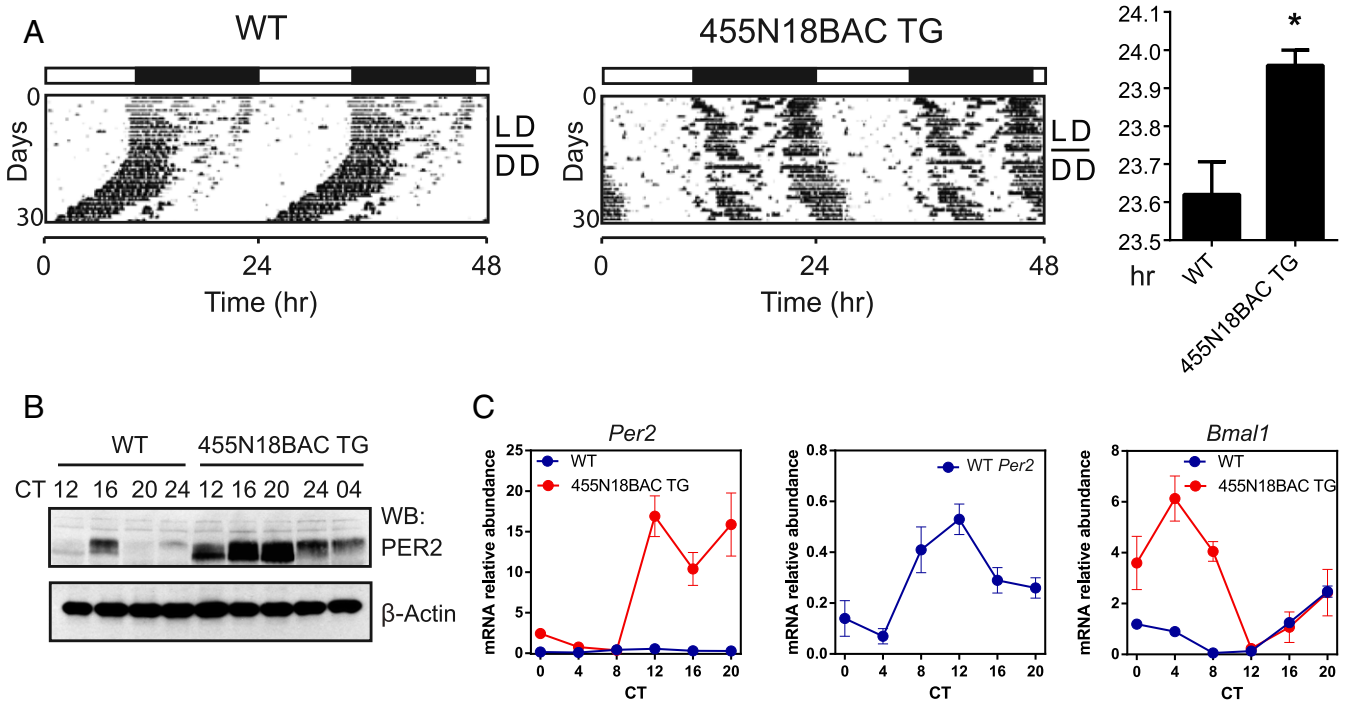

Fig. 6. Rhythmic PER2 overexpression in Per2 BAC transgenic (TG) mice lengthened circadian activity period and increased *Bmal1* circadian amplitude. (*A*) Representative locomotor activity records from WT and *455N18BAC* TG mice. Animals were maintained on LD12:12 for the first 12 d, indicated by the filled and empty bars *Above* the records, before transfer to DD to measure free-running period. The 455N18BAC TG mice exhibited significantly longer free-running periods than WT mice (23.96 ± 0.0400 vs. 23.62 ± 0.08602, $n = 5$, t test: $P = 0.0071$). (*B*) PER2 proteins are rhythmically overexpressed in 455N18BAC TG. Western blotting was performed using total protein extracts from liver with the PER2 antibody. (*C*) Real-time RT-PCR analysis of Per2 and Bmal1 expression in liver tissues from WT and *455N18BAC* TG mice. (*Left*) *Per2* mRNA level from 455N18BAC TG samples (red circles) were significantly elevated (two-way ANOVA, $P < 0.0001$) compared with the WT control (blue circles, *Middle*). (*Right*) *Bmal1* mRNA level from 455N18BAC TG samples (red circles) were also significantly elevated (two-way ANOVA, $P < 0.0001$) compared with the WT control.

the effects of rhythmic PER2 overexpression on circadian behavior and gene expression.

***Per2::LucSV* Showed Enhanced Temperature Compensation in Tissue Clocks Compared with *Per2::Luc*.** Temperature compensation is a defining feature of the circadian clock, evolved to maintain consistent periodicity over temperature fluctuation in daily and seasonal cycles (1). Previously, we employed *Per2::Luc* mice and showed that circadian rhythms in peripheral tissues are temperature compensated (43). To examine whether the enhanced central and peripheral circadian clocks in *Per2::LucSV* display varying temperature compensation relative to *Per2::Luc*, we harvested SCN and peripheral tissue explants from *Per2::LucSV* heterozygous mice, recorded reporter luminescence rhythms at temperatures ranging between 31 °C and 37 °C, and calculated the average periods for individual tissues. SCN and peripheral tissues from *Per2::LucSV* showed clear temperature compensation; however, compared with *Per2::Luc* (data adopted from ref. 43), *Per2::LucSV* tissues exhibited Q10 values closer to 1.0 than those of *Per2::Luc*, suggesting a more robust temperature compensation in the former (Fig. S7). The largest differences between the Q10 values of the two lines were observed in cornea and lung, while the other four tissues displayed more subtle differences.

Discussion

Posttranscriptional 3′-UTR regulation of *Per2* gene expression as revealed by the *Per2::LucSV* circadian reporter mouse showed lengthened circadian period lengths, greater phase responses to light pulse, and enhanced temperature compensation. Molecular analysis of *Per2::LucSV* revealed elevated abundance and oscillatory amplitude of PER2 as well as several other circadian components, suggesting a functional link between molecular amplitude enhancement and changes in circadian behavioral rhythms. In addition, we found a pivotal role of miR-24 in *Per2* expression, providing a mechanistic explanation for the enhanced PER2 levels and circadian amplitude. Finally, we found that PER2 protein accumulation activates its own expression, supporting a positive role for PER2 in circadian transcription. These results highlight the multifunctional roles of PER2 within the circadian clock mechanism.

Our studies on the enhanced rhythms in *Per2::LucSV* revealed important miRNA regulation of PER2 expression and circadian rhythms. Specifically, mapping of the 3′-UTR identified a miR-24 binding site, and cellular functional assays showed a dominant role of miR-24 in PER2 expression. In comparison, miR-30 seems to play a less prominent role, as a mutation in the miR-30 site only weakly enhanced reporter expression. Previously, 248 mRNAs were found to be down-regulated by miR-24 overexpression, and *Per2* is among the gene targets with a miR-24 seed sequence (44). On the other hand, no other miR-24 target genes identified therein are known to regulate PER2 protein level directly. A recent study (29) also implicated both miR-24 and miR-30 in PER2 expression; our results further define their relative contribution. Contrary to the period shortening observed in global *Dicer* knockout mice (29), both *Per2::LucSV* and *455N18BAC Per2* TG mice with rhythmic PER2 overexpression showed lengthened circadian periods, suggesting confounding effects of other miRNAs (in addition to miR-24 and miR-30a) on PER2 expression and circadian periodicity. Previously, the miR-192/194 cluster has been shown to coordinately repress expression of all three *Per* genes; similar to the role of miR-24 reported here (Fig. 4), expression of miR-192/194 in NIH 3T3 cells shortened the circadian period (45). Apart from circadian period, miRNAs have also been found to modulate oscillatory

amplitude. For example, a miRNA overexpression screen identified miR-276a as a clock-related miRNA expressed in fly head (46). Deregulation of miR-276a expression, either up or down, in clock neurons attenuated circadian rhythmicity. The *Timeless* gene, playing an important role in the negative loop of *Drosophila* oscillator, was identified as a direct target of miR-276a and disruption of the cognate binding site on *Timeless* 3′-UTR elevated TIM protein levels. However, unlike PER2 overexpression in our study, TIM accumulation due to the miR-276a binding site mutation led to behavioral arrhythmicity. These studies together indicate important yet diverse roles of miRNAs in circadian clock regulation.

PER proteins are central circadian components with important roles in (patho)physiology (47, 48), yet their mechanistic functions are not fully understood. Previously, constitutive overexpression of PER2 was found to disrupt the clock in fibroblasts and tissues (10); in contrast, *Per2::LucSV* mice maintain high-amplitude oscillation of overexpressed PER2 and correspondingly show robust behavioral rhythms. These results suggest that rhythmic accumulation, rather than expression level per se, of PER2 is critical for circadian oscillation. Our results also provide in vivo evidence for a positive role of PER2 in the circadian oscillator. In a canonical model, PER proteins are believed to play a requisite role in nuclear translocation of CRYs as well as the subsequent transcriptional repression (2, 7). On the other hand, biochemical/molecular and in vivo evidence has also shown that PERs can function as positive factors to enhance E-box induction (11–14, 42). Complementing the mouse loss-of-function studies where *Per* knockout mice displayed reduced *Per* expression (48, 49), our current work provides an in vivo gain-of-function context highlighting a positive role of PER2 in circadian transcription. Our results showed reduced *Rev-Erbα* transcript levels in both *Per2::LucSV* and *455N18BAC* TG, suggesting that PER2 may repress the E-box–driven *Rev-Erbα* transcription, thus relieving REV-ERB repression of circadian genes. Other mechanisms are also possible. It was recently shown that PER1/2 interfere with CRY interaction with CLOCK/BMAL1 immediately following translocation to the nucleus, causing delay of CRY-mediated repression (12). Consistent with the notion that such phase delay is required for the circadian period length (13), *Per2::LucSV* mice displayed longer period length (~24.0 h) potentially attributable to heightened PER2 levels and activating activities. Alternative mechanisms for PER2 regulation of circadian periodicity are also possible. For example, prolonged degradation arising from the higher abundance of PER2 in *Per2::LucSV* mice could also contribute to circadian period lengthening. Moreover, in the aforementioned study (29), the period shortening in *Dicer* knockout mice was attributed to the ascending phase of the circadian cycle, specifically correlating with the accelerated cytoplasmic accumulation of PER2. Further studies are required to integrate PER2 expression, cellular localization, dual activity, and phosphorylation-coupled turnover in the circadian clock mechanism.

Per2::LucSV cells, displaying three- to fourfold enhancement in reporter bioluminescence over *Per2::Luc*, are ideally suited for high-sensitivity applications such as single-cell or microplate circadian monitoring (36, 37). *Per::LucSV* mice also represent an excellent in vivo model to understand regulation of circadian amplitude. While robust amplitude has clear health implications as chronic diseases and aging are known to correlate with damped circadian amplitude (50–52), the molecular mechanisms underlying circadian amplitude regulation are not well understood, mainly involving REV-ERBs and RORs in the secondary loop (17–19). The current study, on the other hand, suggests the core loop factor PER2 functions as a regulator of circadian amplitude. The positive role of PER2 in circadian transcription is in agreement with a functional plasticity of this pivotal core clock component (12). The ability to "buffer" or modulate the antagonism between CLOCK/BMAL1 and CRY may place PER2 in a unique position to modulate amplitude. The clock is inherently a self-limiting, rhythmic machinery, known as a "limit cycle" (53). Measures that perturb the positive–negative arm balance beyond a homeostatic range will conceivably damp the overall amplitude of the following cycles. This notion is supported by a stoichiometric ratio between the positive and negative core factors in fibroblast cells (54), as well as recent studies showing that a clock-enhancing compound only moderately enhances ROR activity and clock output gene expression (55–57). A possible dual role of PER proteins affords a built-in modulatory mechanism in the core loop, bridging the two competing arms and conferring functional dexterity to ensure clock robustness.

The circadian clock is highly sensitive to temperature changes (58), yet it is also imperative that the circadian period is temperature compensated such that constant periodicity is maintained despite environmental fluctuations (1). Temperature compensation has been described in various experimental systems (59–62), and several studies highlighted a mechanistic role of phosphorylation in temperature compensation. For example, casein kinase 1 (CK1), a key enzyme targeting PER proteins, has been shown to be relatively temperature insensitive (59). A recent study (63) employed both computational modeling and biochemical assays to demonstrate that PER2 protein stability, and therefore its level and activity, is regulated by a two-site phosphoswitch controlled by CK1 and a more temperature-sensitive priming kinase. The phosphoswitch was shown to regulate the mode of PER2 phosphorylation-dependent degradation, thereby enabling constant periodicity under varying temperatures. In the current study, *Per2::LucSV* mice showed a more robust temperature compensation compared with *Per2::Luc* (43), as evidenced by Q10 values from *Per2::LucSV* tissue clocks that were closer to 1. Future studies will examine whether the elevated PER2 levels directly impinge on temperature compensation through the phosphoswitch mechanism.

In conclusion, we generated a circadian reporter mouse line, *Per2::LucSV*, expressing high levels of PER2::LUC fusion proteins. Mechanistic studies revealed key regulatory functions of the *Per2* 3′-UTR and PER2 proteins in core circadian oscillators. The high-amplitude rhythms also render *Per2::LucSV* mice a useful research tool for future function and mechanism studies.

Materials and Methods

The *Per2::LucSV* knockin targeting vector was derived from the backbone of *Per2::Luc* targeting vector with modifications. The 455N18BAC *Per2* TG mice were generated as previously described by using the *455N18BAC* clone, which covers the *Per2* genomic locus (64). Animal husbandry for all of the studies was carried out under Institutional Animal Care and Use Committee guidelines and the procedures were conducted as described in animal protocols approved by Northwestern University, Vanderbilt University, The University of Texas Southwestern Medical Center at Dallas, and The University of Texas Health Science Center at Houston (UTHSC-H). The ligation-mediated (LM)-PAT was performed as described previously (36) with slight modifications. *Per2::Luc* and *Per2::LucSV* MEFs were isolated from 12.5 d postcoitum (DPC) embryos and immortalized (23). Circadian gene expression (23, 65) and temperature compensation (39) experiments were performed as described. Data are presented as means ± SEM. $P < 0.05$ was considered statistically significant. For details regarding transgenic mice, tissue explant cultures, mRNA and protein analysis, plasmids and small hairpin RNAs, cell culture and reporter assays, please refer to *SI Materials and Methods*.

ACKNOWLEDGMENTS. We thank A. L. Joyner for providing W4 ES cells, L. Doglio for performing ES cell microinjections, I. Kornblum and J.-H. Choe for technical support, and other members of the S.-H.Y. and J.S.T. laboratories for advice and discussion. This work was supported in part by NIH/National Institute of General Medical Sciences (NIGMS) Grant R01GM114424 (to S.-H.Y.); The Welch Foundation, AU-1731 and NIH/National Institute on Aging Grants R01AG045828 and R01AG045828-04S1 (to Z.C.); NIH Grant NS099813 (to C.L.); NARSAD Young Investigator Grant 21267, the Sumitomo Foundation Grant for Basic Science Research Projects 150056, and the Tomizawa Jun-ichi & Keiko Fund of Molecular Biology Society of Japan for Young Scientists (to S.K.); Japan Society for the Promotion of Science (JSPS) KAKENHI JP26293048, the Uehara Memorial Foundation (to N.K.); JSPS 15H04683 and JSPS 16H01880 (to K.Y.);

NIH/NINDS NS051278 (to S.Y.); NIH/NIGMS R01GM112991 and R01GM111387 (to C.B.G.); and NIH/National Institute of Mental Health (NIMH) Silvio O. Conte Center P50MH074924 and NIH/NIMH U01MH61915 (to J.S.T.). J.S.T. is an Investigator in the Howard Hughes Medical Institute, and a cofounder and Scientific Advisory Board member of Reset Therapeutics, Inc., a biotech company working on circadian rhythms and metabolism.

1. Pittendrigh CS (1960) Circadian rhythms and the circadian organization of living systems. *Cold Spring Harb Symp Quant Biol* 25:159–184.
2. Takahashi JS, Hong HK, Ko CH, McDearmon EL (2008) The genetics of mammalian circadian order and disorder: Implications for physiology and disease. *Nat Rev Genet* 9:764–775.
3. Hardin PE, Panda S (2013) Circadian timekeeping and output mechanisms in animals. *Curr Opin Neurobiol* 23:724–731.
4. Herzog ED, Hermanstyne T, Smyllie NJ, Hastings MH (2017) Regulating the suprachiasmatic nucleus (SCN) circadian clockwork: Interplay between cell-autonomous and circuit-level mechanisms. *Cold Spring Harb Perspect Biol* 9:a027706.
5. Takahashi JS (2017) Transcriptional architecture of the mammalian circadian clock. *Nat Rev Genet* 18:164–179.
6. Kume K, et al. (1999) mCRY1 and mCRY2 are essential components of the negative limb of the circadian clock feedback loop. *Cell* 98:193–205.
7. Reppert SM, Weaver DR (2002) Coordination of circadian timing in mammals. *Nature* 418:935–941.
8. Yagita K, et al. (2000) Dimerization and nuclear entry of mPER proteins in mammalian cells. *Genes Dev* 14:1353–1363.
9. Yagita K, et al. (2002) Nucleocytoplasmic shuttling and mCRY-dependent inhibition of ubiquitylation of the mPER2 clock protein. *EMBO J* 21:1301–1314.
10. Chen R, et al. (2009) Rhythmic PER abundance defines a critical nodal point for negative feedback within the circadian clock mechanism. *Mol Cell* 36:417–430.
11. Hampp G, et al. (2008) Regulation of monoamine oxidase A by circadian-clock components implies clock influence on mood. *Curr Biol* 18:678–683.
12. Akashi M, et al. (2014) A positive role for PERIOD in mammalian circadian gene expression. *Cell Rep* 7:1056–1064.
13. Ogawa Y, et al. (2011) Positive autoregulation delays the expression phase of mammalian clock gene Per2. *PLoS One* 6:e18663.
14. Ye R, Selby CP, Ozturk N, Annayev Y, Sancar A (2011) Biochemical analysis of the canonical model for the mammalian circadian clock. *J Biol Chem* 286:25891–25902.
15. Preitner N, et al. (2002) The orphan nuclear receptor REV-ERBalpha controls circadian transcription within the positive limb of the mammalian circadian oscillator. *Cell* 110: 251–260.
16. Sato TK, et al. (2004) A functional genomics strategy reveals Rora as a component of the mammalian circadian clock. *Neuron* 43:527–537.
17. Hogenesch JB, Herzog ED (2011) Intracellular and intercellular processes determine robustness of the circadian clock. *FEBS Lett* 585:1427–1434.
18. Zhao X, et al. (2016) Circadian amplitude regulation via FBXW7-targeted REV-ERBα degradation. *Cell* 165:1644–1657.
19. Zhu B, et al. (2015) Coactivator-dependent oscillation of chromatin accessibility dictates circadian gene amplitude via REV-ERB loading. *Mol Cell* 60:769–783.
20. Gallego M, Virshup DM (2007) Post-translational modifications regulate the ticking of the circadian clock. *Nat Rev Mol Cell Biol* 8:139–148.
21. Kojima S, Shingle DL, Green CB (2011) Post-transcriptional control of circadian rhythms. *J Cell Sci* 124:311–320.
22. Lim C, Allada R (2013) Emerging roles for post-transcriptional regulation in circadian clocks. *Nat Neurosci* 16:1544–1550.
23. Yoo SH, et al. (2013) Competing E3 ubiquitin ligases govern circadian periodicity by degradation of CRY in nucleus and cytoplasm. *Cell* 152:1091–1105.
24. Lee J, et al. (2008) Dual modification of BMAL1 by SUMO2/3 and ubiquitin promotes circadian activation of the CLOCK/BMAL1 complex. *Mol Cell Biol* 28:6056–6065.
25. Reischl S, Kramer A (2011) Kinases and phosphatases in the mammalian circadian clock. *FEBS Lett* 585:1393–1399.
26. Cardone L, et al. (2005) Circadian clock control by SUMOylation of BMAL1. *Science* 309:1390–1394.
27. Mehta N, Cheng HY (2013) Micro-managing the circadian clock: The role of microRNAs in biological timekeeping. *J Mol Biol* 425:3609–3624.
28. Fabian MR, Sonenberg N, Filipowicz W (2010) Regulation of mRNA translation and stability by microRNAs. *Annu Rev Biochem* 79:351–379.
29. Chen R, D'Alessandro M, Lee C (2013) miRNAs are required for generating a time delay critical for the circadian oscillator. *Curr Biol* 23:1959–1968.
30. Kadener S, et al. (2009) A role for microRNAs in the Drosophila circadian clock. *Genes Dev* 23:2179–2191.
31. Kojima S, Gatfield D, Esau CC, Green CB (2010) MicroRNA-122 modulates the rhythmic expression profile of the circadian deadenylase Nocturnin in mouse liver. *PLoS One* 5: e11264.
32. Luo W, Sehgal A (2012) Regulation of circadian behavioral output via a microRNA-JAK/STAT circuit. *Cell* 148:765–779.
33. Cheng HY, et al. (2007) microRNA modulation of circadian-clock period and entrainment. *Neuron* 54:813–829.
34. Yoo SH, et al. (2004) PERIOD2:LUCIFERASE real-time reporting of circadian dynamics reveals persistent circadian oscillations in mouse peripheral tissues. *Proc Natl Acad Sci USA* 101:5339–5346.
35. Yoo SH, et al. (2005) A noncanonical E-box enhancer drives mouse Period2 circadian oscillations in vivo. *Proc Natl Acad Sci USA* 102:2608–2613.
36. Welsh DK, Yoo SH, Liu AC, Takahashi JS, Kay SA (2004) Bioluminescence imaging of individual fibroblasts reveals persistent, independently phased circadian rhythms of clock gene expression. *Curr Biol* 14:2289–2295.
37. Chen Z, et al. (2012) Identification of diverse modulators of central and peripheral circadian clocks by high-throughput chemical screening. *Proc Natl Acad Sci USA* 109: 101–106.
38. Sallés FJ, Strickland S (1999) Analysis of poly(A) tail lengths by PCR: The PAT assay. *Methods Mol Biol* 118:441–448.
39. Kojima S, Green CB (2015) Analysis of circadian regulation of poly(A)-tail length. *Methods Enzymol* 551:387–403.
40. Kojima S, Sher-Chen EL, Green CB (2012) Circadian control of mRNA polyadenylation dynamics regulates rhythmic protein expression. *Genes Dev* 26:2724–2736.
41. Lewis BP, Burge CB, Bartel DP (2005) Conserved seed pairing, often flanked by adenosines, indicates that thousands of human genes are microRNA targets. *Cell* 120: 15–20.
42. Miki T, et al. (2012) PML regulates PER2 nuclear localization and circadian function. *EMBO J* 31:1427–1439.
43. Reyes BA, Pendergast JS, Yamazaki S (2008) Mammalian peripheral circadian oscillators are temperature compensated. *J Biol Rhythms* 23:95–98.
44. Lal A, et al. (2009) miR-24 inhibits cell proliferation by targeting E2F2, MYC, and other cell-cycle genes via binding to "seedless" 3′UTR microRNA recognition elements. *Mol Cell* 35:610–625.
45. Nagel R, Clijsters L, Agami R (2009) The miRNA-192/194 cluster regulates the Period gene family and the circadian clock. *FEBS J* 276:5447–5455.
46. Chen X, Rosbash M (2016) mir-276a strengthens Drosophila circadian rhythms by regulating timeless expression. *Proc Natl Acad Sci USA* 113:E2965–E2972.
47. Fu L, Pelicano H, Liu J, Huang P, Lee C (2002) The circadian gene Period2 plays an important role in tumor suppression and DNA damage response in vivo. *Cell* 111: 41–50.
48. Bae K, et al. (2001) Differential functions of mPer1, mPer2, and mPer3 in the SCN circadian clock. *Neuron* 30:525–536.
49. Zheng B, et al. (2001) Nonredundant roles of the mPer1 and mPer2 genes in the mammalian circadian clock. *Cell* 105:683–694.
50. Green CB, Takahashi JS, Bass J (2008) The meter of metabolism. *Cell* 134:728–742.
51. Schroeder AM, Colwell CS (2013) How to fix a broken clock. *Trends Pharmacol Sci* 34: 605–619.
52. Nohara K, Yoo SH, Chen ZJ (2015) Manipulating the circadian and sleep cycles to protect against metabolic disease. *Front Endocrinol (Lausanne)* 6:35.
53. Schibler U, Naef F (2005) Cellular oscillators: Rhythmic gene expression and metabolism. *Curr Opin Cell Biol* 17:223–229.
54. Lee Y, Chen R, Lee HM, Lee C (2011) Stoichiometric relationship among clock proteins determines robustness of circadian rhythms. *J Biol Chem* 286:7033–7042.
55. He B, et al. (2016) The small molecule nobiletin targets the molecular oscillator to enhance circadian rhythms and protect against metabolic syndrome. *Cell Metab* 23: 610–621.
56. Nohara K, et al. (2015) Ammonia-lowering activities and carbamoyl phosphate synthetase 1 (Cps1) induction mechanism of a natural flavonoid. *Nutr Metab (Lond)* 12:23.
57. Gloston GF, Yoo SH, Chen ZJ (2017) Clock-enhancing small molecules and potential applications in chronic diseases and aging. *Front Neurol* 8:100.
58. Buhr ED, Yoo SH, Takahashi JS (2010) Temperature as a universal resetting cue for mammalian circadian oscillators. *Science* 330:379–385.
59. Isojima Y, et al. (2009) CKIepsilon/delta-dependent phosphorylation is a temperature-insensitive, period-determining process in the mammalian circadian clock. *Proc Natl Acad Sci USA* 106:15744–15749.
60. Chen Z, McKnight SL (2007) A conserved DNA damage response pathway responsible for coupling the cell division cycle to the circadian and metabolic cycles. *Cell Cycle* 6: 2906–2912.
61. Mehra A, et al. (2009) A role for casein kinase 2 in the mechanism underlying circadian temperature compensation. *Cell* 137:749–760.
62. Portolés S, Más P (2010) The functional interplay between protein kinase CK2 and CCA1 transcriptional activity is essential for clock temperature compensation in Arabidopsis. *PLoS Genet* 6:e1001201.
63. Zhou M, Kim JK, Eng GW, Forger DB, Virshup DM (2015) A Period2 phosphoswitch regulates and temperature compensates circadian period. *Mol Cell* 60:77–88.
64. Antoch MP, et al. (1997) Functional identification of the mouse circadian clock gene by transgenic BAC rescue. *Cell* 89:655–667.
65. Jeong K, et al. (2015) Dual attenuation of proteasomal and autophagic BMAL1 degradation in Clock Δ19/+ mice contributes to improved glucose homeostasis. *Sci Rep* 5:12801.